ISSN 8755-6839

SCIENCE OF **TSUNAMI HAZARDS**

Journal of Tsunami Society International

Volume 36 **Number 3** **2017**

MANIFESTATION OF THE 1963 URUP TSUNAMI ON SAKHALIN: OBSERVATIONS AND MODELING

Andrey Zaytsev[1,2)], Irina Kostenko[1)], Andrey Kurkin[2,3)], Efim Pelinovsky[2,4,5)] & George Pararas-Carayannis [6]

1) Special Research Bureau for Automation of Marine Researches, Yuzhno-Sakhalinsk, Russia
2) Nizhny Novgorod State Technical University n.a. R. Alekseev, Nizhny Novgorod, Russia
3) Institute of Space Technologies, Peoples' Friendship University of Russia (RUDN University), Moscow, Russia
4) Institute of Applied Physics, Nizhny Novgorod, Russia
5) National Research University – Higher School of Economics, Moscow, Russia
6) Tsunami Society International, Honolulu, Hawaii, USA.

ABSTRACT

In the history of instrumental observations, the tsunami of 1963 generated in the vicinity of Urup in the Kuril Islands had the highest runup heights on the coasts of Sakhalin Island. It was generated by a strong earthquake which had a moment magnitude M_w 8.1. The present study summarizes the known observations of this event along the coasts of Sakhalin, in the Hawaiian Islands and elsewhere in the Pacific Ocean. Additionally, the prestent study includes the numerical simulation of this 1963 tsunami event in the framework of nonlinear shallow water theory. The results of the numerical calculations are in good agreement with the observational data.

1. INTRODUCTION

Sakhalin Island is located in the Sea of Okhotsk, which is in the northwestern part of the Pacific Ocean and is connected to the Pacific Ocean by the straits of the Kuril Islands (Fig. 1). The width of the Kuril Islands is about 500 km and the length is about 1200 km, which is 41.6% of the total distance between the Kamchatka Peninsula and the island of Hokkaido. The Pacific and the Kuril Islands are located along a strong seismic activity zone where major and great earthquakes occur, and which can generate destructive tsunamis across the Pacific Ocean basin. Tsunamis originating from distant Pacific sources upon entering the Sea of Okhotsk become weakened due to the shielding effect of the Kuril Islands (Kostenko et al, 2016, Shevchenko et al., 2011). On the other hand, earthquakes originating in the Sea of Okhotsk and the Sea of Japan can generate tsunamis which can impact significantly the Island of Sakhalin. It should be noted that the network of tide gauges established along coastal areas of Sakhalin Island, have provided valuable historical data of tsunamis for the last 60 years. For that period, a total of about 30 tsunamis were recorded. (Kostenko et al, 2015, Zaytsev et al., 2017). The magnitudes of earthquakes that have generated tunamis on Sakhalin over the past 100 years, usually exceed M_s 6.1, while maximum magnitudes exceeded $M_s = 9$ for two events (Chile, 1960 and Japan, 2011).

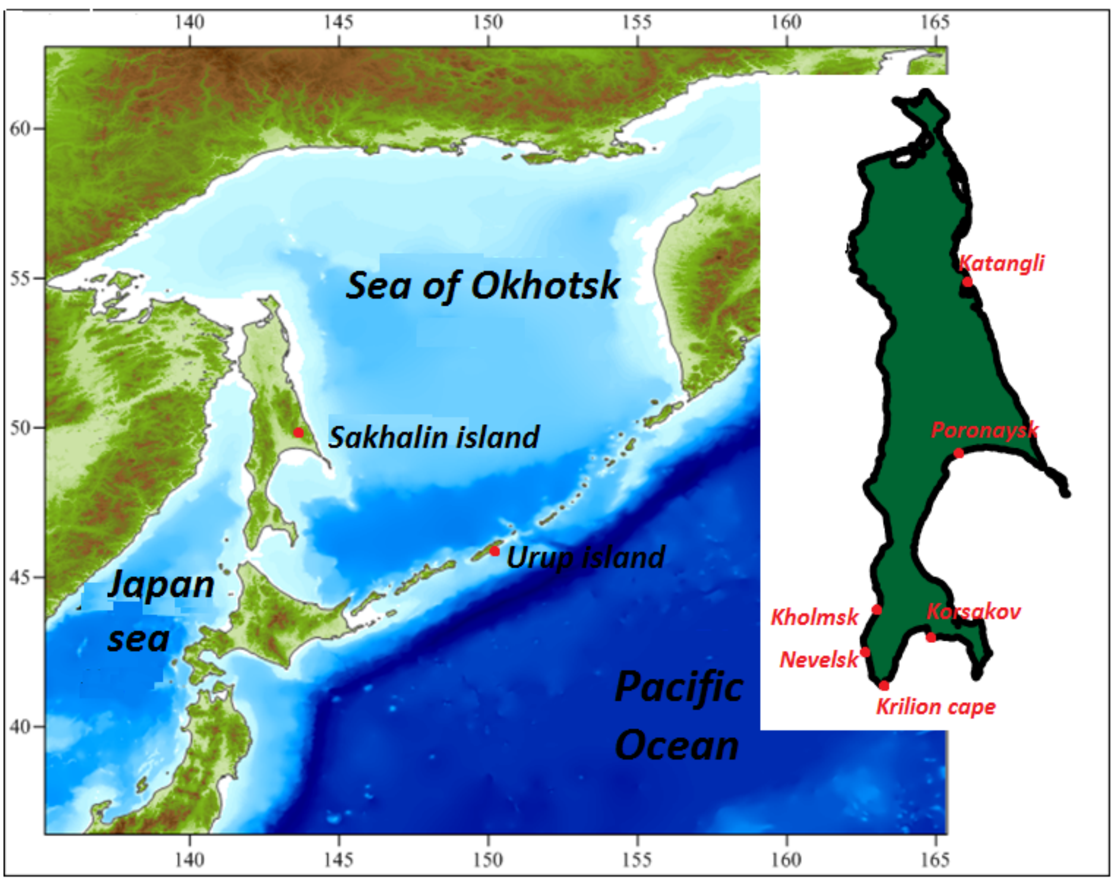

Figure 1. Sakhalin Island

Inpite of the fact that in the Far Eastern region earthquakes with magnitudes of more than M_s 8 over the past 100 years have occurred, there has been no catastrophic tsunami with losses of human lives on Sakhalin Island. However, though the maximum tsunami height did not exceed 2-3 m for these large events, such runup heights were sufficient to cause damage on Sakhalin's infrastructure. For example, during the Nevel earthquake of August 2, 2007 (magnitude M = 6.2), the seabed rose, so it became necessary to rebuild the port (Zaitsev et al, 2008, 2009). Fig. 2 shows the location of tsunami sources that have been detected on Sakhalin Island over the past 300 years. The figure identifies the main areas of tsunami generation. Most of the sources were located relatively close to Sakhalin, along the northern and eastern part of the Sea of Japan or along the Pacific coast of the southern and central Kuril Islands. For example, the severe earthquake of March 11, 2011, east of Honshu Island in Japan, caused not only a devastating tsunami in Japan and elsewhere in the Pacific but also led to the destruction of the coastal ice field in the Kuril Islands (Kaistrenko et al, 2013).

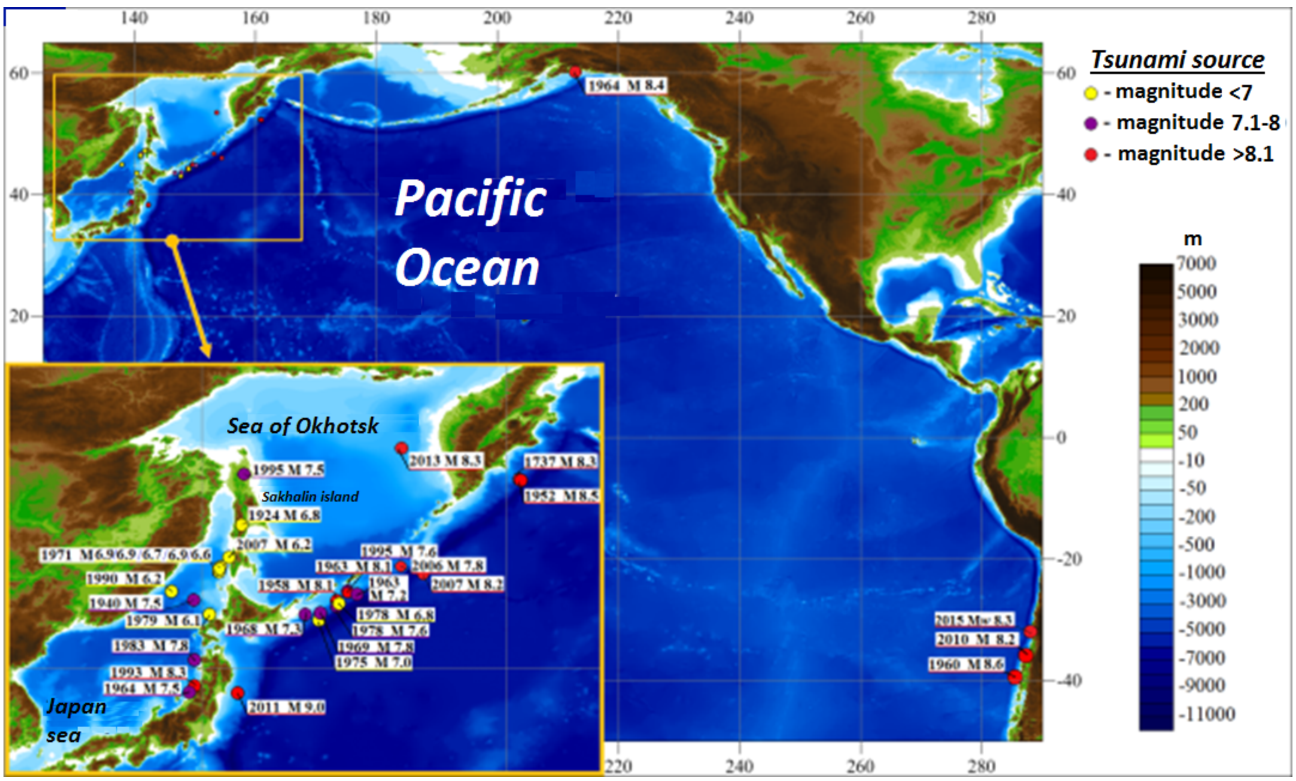

Figure 2. Epicenters of earthquakes that caused tsunami, which manifested themselves on the coast of Sakhalin

In summary, the Kuril Islands can be impacted not only from tsunamis generated from distant sources, but also from locally generated events. The strongest impact on Sakhalin was caused by the tsunami generated by the earthquake of October 13, 1963 at 05:17:51 (Greenwich Mean Time) near the area of Urup Island (Fig. 1)(. The moment magnitude (M_w) of this earthquake was estimated to be 8.1, (but according to some data, it may have been as much as M_w = 8.5). The tsunami source area was near the wider straits of Vries and Bussol, thus contributing to a greater amount of tsunami energy entering the Sea of Okhotsk. The present study presents a discussion of the 1963 Urup tsunami observations on Sakhalin Island and elsewhere, as well as to the numerical modeling of this event.

2. TECTONIC SETTING OF THE KURIL ISLAND REGION

In order to understand the generation of tsunamigenic earthquakes near the Kuril Islands and the Sea of Okhotsk, there is a need for a brief review of the seimo-tectonics of the region. This is necessary as the overall tectonics of northeast Asia are very complicated and not sufficiently understood. For example, it has not been determined with certainty whether the Sea of Okhotsk and the northern Japanese islands are part of the North American plate or of a separate Okhotsk tectonic plate. On the Pacific Ocean side, earthquake slip vectors along the Kuril and Japan trenches are consistent with either a Pacific-North America or a Pacific-Okhotsk plate motion. However, it has been concluded that the Pacific-North America plate motion is better supported (Pararas-Carayannis, 1994, 2006).

Furthermore, the volcanic Kuril island arc chain runs from the northern tip of the Japanese Island of Hokkaido to the southern tip of Russia's Kamchatka Peninsula. It is also a region of high seismic activity. The Kuril Trench has been formed by the subduction of the Pacific plate under the North American plate and extends from the offshore central area of Kamchatka to Hokkaido.

The plate tectonics of the Southern Kuril islands-Northern Hokkaido region are also quite different than those along the southern portion of the Japanese Trench. The South Kuril Islands are part of the Kuril arc in the Okhotsk plate which has been colliding westward against the Northeast Japan arc, along the Hidaka Collision Zone (HCZ), where new continental crust is created by active arc-arc collision (Pararas-Carayannis, 1994, 2006).

Also, deep seismic reflection studies (Ito, Kazuka @Abe, 2001) show the lower crust of the Kuril arc to be delaminated at a depth of about 23 km. These studies indicate that the upper half (above 23 km) - consisting of the earth's upper crust and the upper portion of lower crust of the Kuril arc - is thrusting over the Northeast Japan arc along the Hidaka Main Thrust (HMT). However, the lower half (below 23 km) - consisting of the lower portion of lower crust and upper mantle material - is descending downward (Pararas-Carayannis, 1994, 2006).

As a result of such kinematic processes, the wedge of the Northeast Japan arc is intruded into the delaminated Kuril arc, as the Pacific plate is subducting northward beneath both of the above mentioned structures, thus continuing the arc-arc collision (and continental crust production). The complex, seismo-tectonic kinematic process of this region has been named "Delamination-wedge-subduction system" - which may apply also to other areas where active arc-arc collision and concurrent subduction take place (Pararas-Carayannis, 2006).

This region of the southern Kuril Islands is characterized by crustal displacements which appear to be ocurring along the boundaries of broken subplates that may not be longer than 200-250 km. The Kuril

Back-Arc basin is a deep basin in southern Sea of Okhotsk, northwest of the Kuril Arc. These fractured smaller plates, near this tectonically active arc-arc collision area, appear to limit the extent of crustal ruptures and therefore the areal extent of tsunami sources. This is the reason why large magnitude earthquakes in this region have generated only locally destructive and not Pacific-wide – tsunamis (Pararas-Carayannis, 1994, 2006).

Specifically, the October 12, 1963 earthquake (as that of October 4, 1994) which ocurred at the Pacific side boundary of the Kuril Arc (near the South Kuril Islands) of the Okhotsk plate. but with lesser vertical subduction and greater rotational movement - as the North Pacific Plate grinds against it. The whole area appears to be highly fractured by complex tectonic interactions and the crustal displacements appear to be ocurring along the boundaries of broken subplates – which as mentioned - may not be longer than 200-250 Km.

3. HISTORICAL DATA ON THE 1963 URUP TSUNAMI

Historical data on tsunami are given in a number of papers (Solovyev, 1965, 1978, Iida et.al, 1967; Pararas-Carayannis, 1968; Pararas-Carayannis & Calebaugh, 1977; Shchetnikov, 1981, 1990; Shevchenko et al., 2012). Tsunami warnings for the Pacific were issued by what was then known as the U. S. Seismic Sea Wave Warning System operated by the Honolulu Observatory in Hawaii for this event and for another potentially tsunamigenic earthquake (Ms 7) near Iturup in the Kurils, a week later (Pararas-Carayannis, 1968; Pararas-Carayannis & Calebaugh, 1977). The earthquake of 13 October, 1963 had a magnitude of 8.1 and occurred at 06:17:51 GMT. The coordinates of the epicenter were 44.81^0N and 149.54^0 (it was on a continental slope near the island of Urup); the focal depth is 47 km.

According to the Urup hydro-meteorological station observations, the tsunami began with the level lowering (the drainage zone was 70-80 m), then came the first wave 2-3 m high. After it a more significant low tide followed, and the drainage region was 400-500 m. The second wave was the most dangerous. Its height, according to the hydrostatic logger in Nevidimka Bay, was 4.4 m. In total, five large waves were observed with an interval of 12-15 minutes, and then the tsunami intensity gradually decreased. The tsunami manifested itself mainly on the Pacific coast of the islands of Urup and Iturup, but also caused quite dangerous fluctuations in sea level in Shikotan, Kunashir (up to 1.5 m), and also on the islands of the Lesser Kuril ridge. On the Middle and Northern Kuril Islands the tsunami was quite intense (about 1 m in height), but it was not dangerous. The tsunami of October, 13 caused significant economic damage to the Kuril Islands facilities (Solovyov, 1965, 1978; Shevchenko et al., 2012). For instance, in the bays of the island of Shikotan several ships were stranded (height up to 2.5 m, current speed up to 10 knots). In many whaling plants on the islands of Urup, Simushir and Iturup the tsunami carried into the sea many tons of coal, fuel and containers.

This tsunami was registered in Japan (maximum height 0.6 m, the tsunami began with a tidal wave), in the Hawaiian Islands (max height up to 0.4 m in Kahului, Island of Maui), in the Aleutian Islands (the height did not exceed 0.4 m), in California (0.5 m) and Mexico (0.7 m) (Iida et.al, 1967; Pararas-Carayannis, 1968; Pararas-Carayannis & Calebaugh, 1977).

On the coast of Sakhalin the tsunami came weakened and the wave heights did not exceed 0.4m (see Table 1), according to observations (the town of Korsakov, Cape Krilion, Katangli settlement). Instrumental ("paper") data on the Sakhalin tsunami recording are shown in Fig. 3. As can be seen, the tsunami waves caused many hours of water level fluctuations, with the first wave not being the maximum.

Table1. The Urup tsunami observations on Sakhalin

Location	Wave height, m	Travel time, hr	Period, min
Katangli	0.4	2.8	23
Poronaisk	0.3	3.3	30
Korsakov	0.4	2.3	25
Cape Krillion	0.4	2.3	8
Nevelsk	0.15		
Kholmsk	0.1		

A week later, on October 20, was recorded the strongest earthquake aftershock with a magnitude of 7.4. A very strong tsunami (up to 15m in height) was observed directly opposite the focus (CapeVan-der-Lind, Urup), outside this zone the wave heights were small. A unique photograph of the tsunami wave which moves down from the coast in Yuzhno-Kurilsk (Kunashir Island) is shown in Fig. 4; the wave height in this bay did not exceed 0.5m.

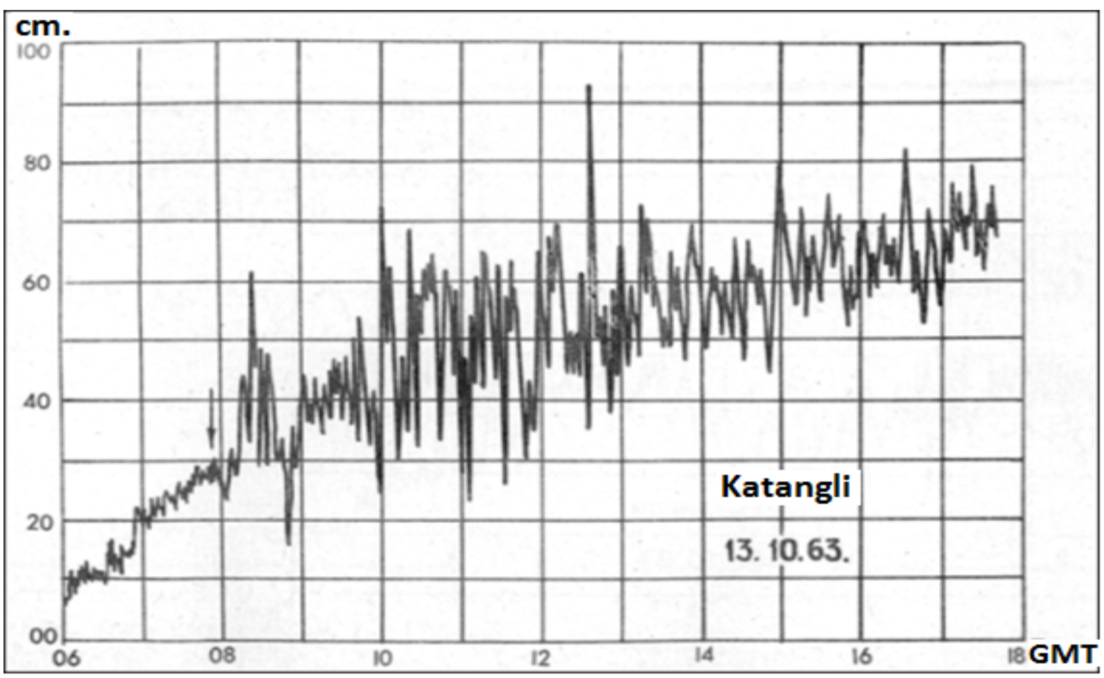

a]

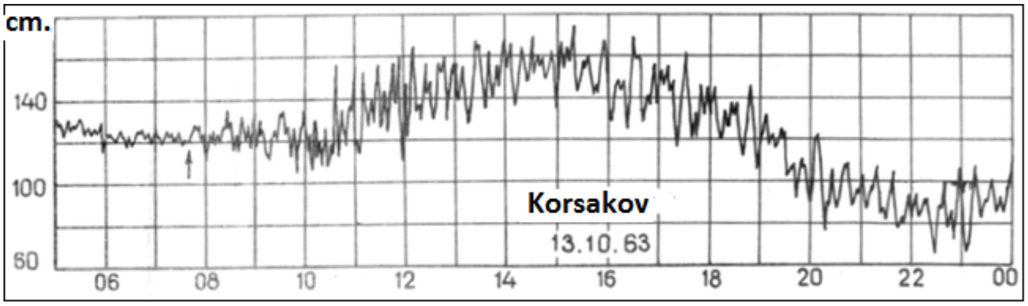

б

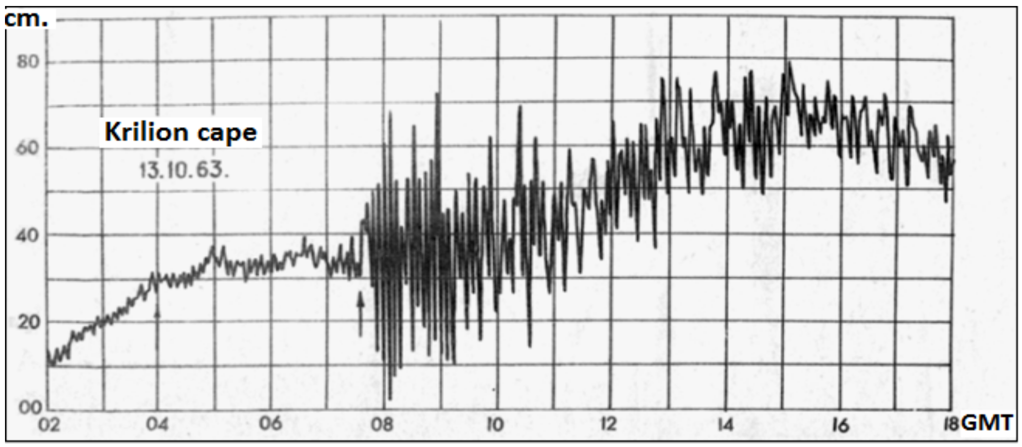

в

Figure 3. Records of the October 13, 1963 tsunami on Sakhalin (*a* - Katangli, *b* - Korsakov, *c* - Cape Krilion) [Schetnikov, 1981, 1990].

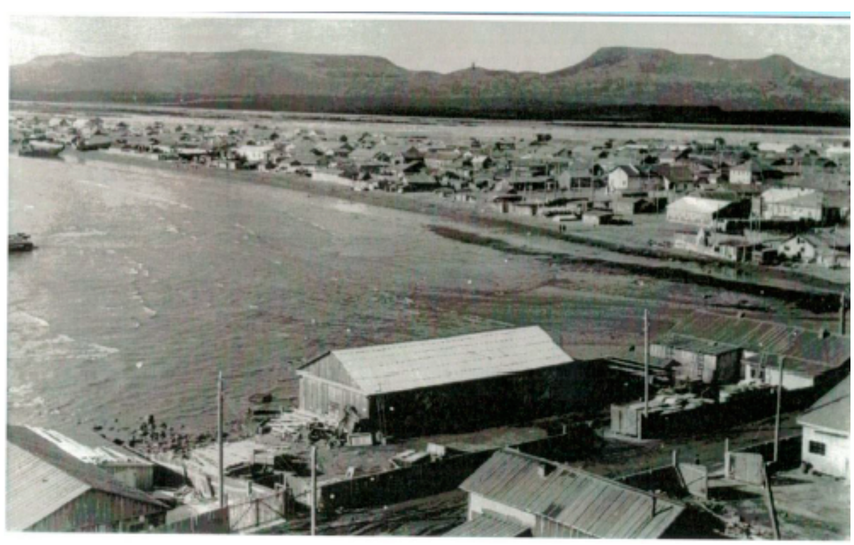

Figure 4.The tsunami wave moves down in Yuzhno-Kurilsk, Kunashir Island on October 20, 1960 (courtesy S.L. Solovyev)

4. MATHEMATICAL MODEL OF THE 1963 TSUNAMI PROPAGATION

Tsunami waves of seismic origin are long waves (the wavelength exceeds the ocean depth), so the based model is the famous non-linear shallow-water theory described by a system of equations, which take into account the sphericity of the Earth, the Coriolis force and the bottom friction (Pelinovsky, 1996, Levin and Nosov, 2016)

$$\frac{\partial M}{\partial t}+\frac{1}{R\cos\theta}\frac{\partial}{\partial\lambda}\left(\frac{M^2}{D}\right)+\frac{1}{R\cos\theta}\frac{\partial}{\partial\theta}\left(\frac{MN\cos\theta}{D}\right)+\frac{gD}{R\cos\theta}\frac{\partial\eta}{\partial\lambda}+\frac{gn^2}{D^{7/3}}M\sqrt{M^2+N^2}=f\,N \quad (1)$$

$$\frac{\partial N}{\partial t}+\frac{1}{R\cos\theta}\frac{\partial}{\partial\lambda}\left(\frac{MN}{D}\right)+\frac{1}{R\cos\theta}\frac{\partial}{\partial\theta}\left(\frac{N^2\cos\theta}{D}\right)+\frac{gD}{R}\frac{\partial\eta}{\partial\theta}+\frac{gn^2}{D^{7/3}}N\sqrt{M^2+N^2}=-f\,M \quad (2)$$

$$\frac{\partial\eta}{\partial t}+\frac{1}{R\cos\theta}\left[\frac{\partial M}{\partial\lambda}+\frac{\partial}{\partial\theta}\left(N\cos\theta\right)\right]=0\,, \quad (3)$$

where η is the sea level displacement with regard to the unperturbed one; *M* and *N* are discharge components along latitude λ and longitude θ; *D* is the basin total depth; *g* is the gravity acceleration, *R* is the Earth radius, *f* is the Coriolis parameter ($f = 2\omega\, sin\theta$), ω is the Earth rotation frequency (rotation period of 24 hours), and *n* is the bottom roughness coefficient. In the calculations, the value $n = 0.015$ $m^{-1/3}s$, typical for the natural bottom (sand, small pebbles) is used. The total basin depth of is defined as:

$$D(\lambda,\theta,t)=h(\lambda,\theta)+\eta(\lambda,\theta,t) \quad (4)$$

,

where *h* is the unperturbed ocean depth, assumed to be known and not changing in time. The bathymetry, created from GEBCO Digital Atlas with a 30 arc second resolution, was used in the calculations[http://www.gebco.net].

The initial conditions correspond to the instantaneous bottom movement

$$\eta(\lambda,\theta,t=0)=\eta_0(\lambda,\theta)\ .\ M(\lambda,\theta,t=0)=N(\lambda,\theta,t=0)=0 \quad . \quad (5)$$

The function $\eta_0\ (\lambda,\theta)$ is found by Okada's solution [Okada, 1985], which determines the residual displacements of the earth surface after the earthquake. This solution is too cumbersome to be given here. It is important to note that the following earthquake parameters are necessary to know for its calculation: fault depth, length (L) and width (W), vertical displacement (D), strike angle (θ), dip angle (δ), slip (rake) angle (λ) - Fig. 5.

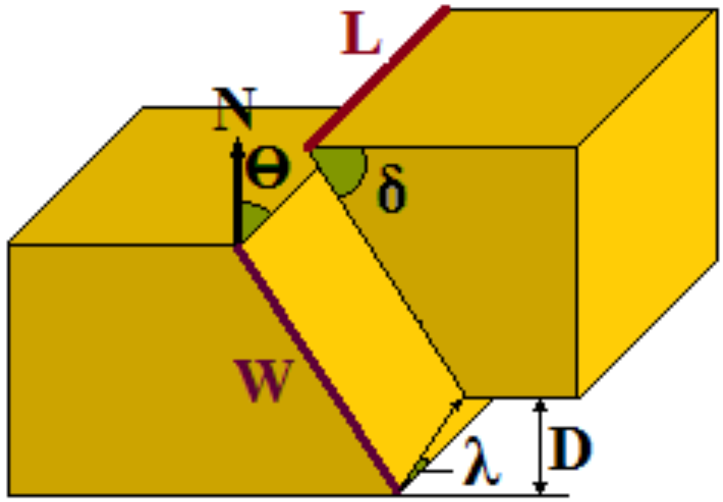

Figure 5.The earthquake parameters

The boundary conditions on the free (sea) boundaries of the computational domain assume the Sommerfeld radiation condition:

$$M_n = \eta\sqrt{gD} \quad (6)$$

where M_n is the normal component of discharge(obviously, this condition requires the smoothness of the computational domain boundary). This condition is exact for shallow water equations ignoring the Coriolis force (the Earth rotation) and the bottom friction. These factors lead to a weak wave reflection from the sea wall and can influence the results of wave parameter calculations at large times when the wave amplitude becomes sufficiently small. In our calculations, the sea boundaries are used in the Pacific to reduce computation time. The sea boundaries are also used in nested grids for calculations in the vicinity of Sakhalin.

The boundary condition on the moving shore is used on the solid walls (coast)

$$D(\lambda, \theta, t) = 0 \quad (7)$$

The NAMI DANCE code of shallow-water equations is used to compute tsunami propagation [http://avi-nami.ce.metu.edu.tr]. It has already been used to model various historical tsunamis [Zaitsev et al., 2005, 2009; Kurkin et al, 2004; Yalciner et al., 2007, 2010; Baranova et al, 2014; Dilmen et al., 2014; Ozer et al. 2015; Zaytsev et al, 2016]. The shallow water equations are solved by a finite-difference method [Shuto et al., 1990; Imamura, 1989]). The NAMI DANCE code includes a subroutine for calculating a tsunami source using Okada formula. It makes it possible to calculate tsunami wave propagation in the water area; wave propagation time and velocity, wave and runup heights, as well as power characteristics [Ozer et al, 2015].The complex control panel view is shown in Fig. 6. The calculation speed depends on the computer capabilities, the step size and other parameters that are set at the start of the calculation.

To compare the numerical results with the observation data, 'computer' tide gauges are located in places closest to the sea level measurement points of the Russian Tsunami Warning Service on Sakhalin Island and the Kuril Islands [http://www.rtws.ru/]. However, they are always located in the open sea, while the real tide gauges are installed in harbor bays, which, in turn, can affect the height and characteristic periods of sea level fluctuations due to resonant (seiche) effects. In general, the bathymetry of the near-shore zone is not set well enough; it does not include port and coastal structures. Therefore, tsunami runup assessments are quite rough for settlements where ports, fish plants and other industrial and civil structures are located.

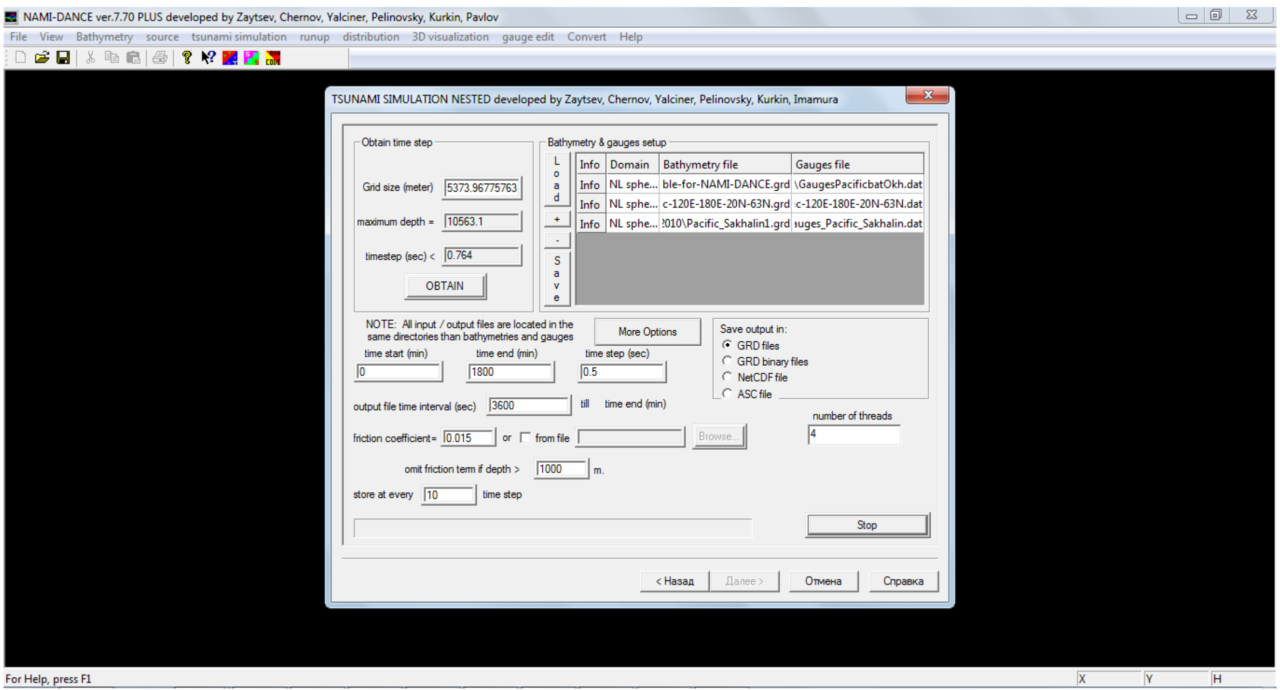

Figure 6. NAMI DANCE complex control panel

5. NUMERICAL MODELING OF THE 1963 URUP TSUNAMI

The results of the 1963 Urup tsunami numerical modeling and its manifestations on the Coast of Sakhalin Island are presented here. It should be reminded that the earthquake had a magnitude of 8.1 (according to some data, Mw = 8.5). The tsunami that was formed as a result of the earthquake, struck the coast of the Kuril Islands with a wave height of about 4 m, and on Sakhalin with a height of 0.4 m. It is an example of one of the most powerful tsunamis that occurred on the Pacific coast of the Kuril Islands during the instrumental measurement period. The tsunami source was located on the Pacific side of Urup near the Vries and Bussol Straits, which contributed to a greater tsunami wave penetration into the Sea of Okhotsk. It was this tsunami that had the strongest impact on Sakhalin.

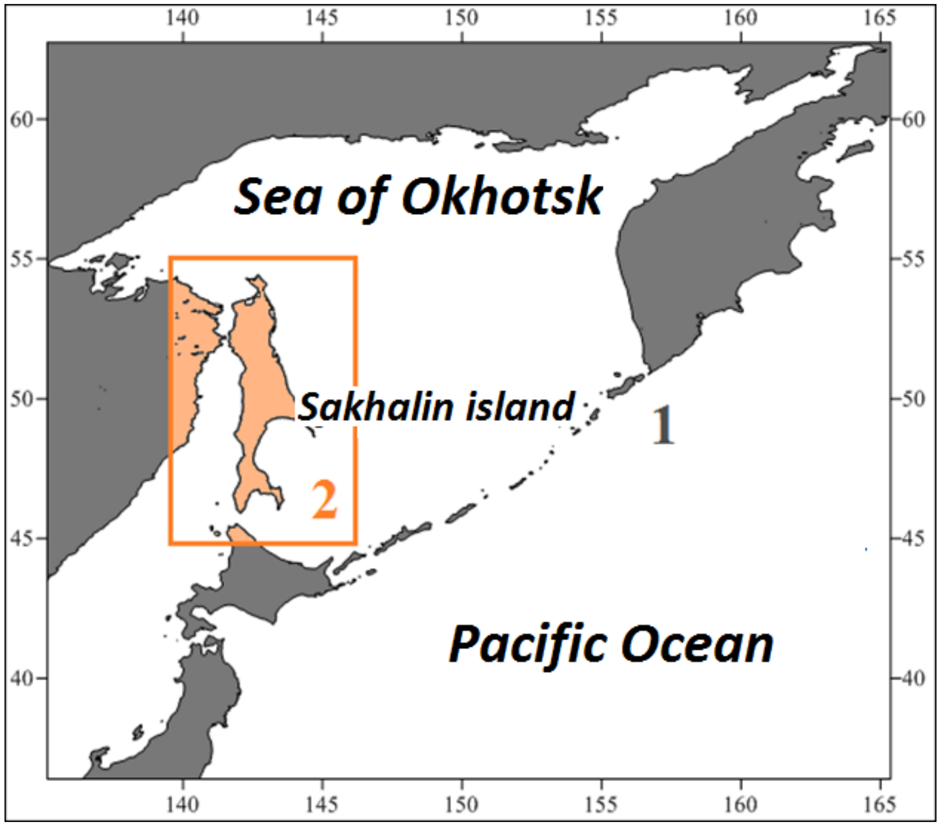

Figure 7. ‘Embedded’ bathymetry used for numerical calculation (**1**- the northwestern area of the Pacific, **2** - the Sakhalin Island region)

Since the tsunami source was located relatively near the coast of Sakhalin, there is no need to calculate tsunami waves throughout the entire Pacific Ocean. The average distance between the nodes of the bathymetry grid in the northwestern Pacific is 690 (541-839) m (Fig. 7). The grid spacing of the ‘embedded’ bathymetry in the vicinity of Sakhalin is 229 (179-279) m.

The 1963 earthquake characteristics are taken from [Ioki and Tanioka, 2008]. They are presented in Table 2.

Table2. October 13, 1963 earthquake parameters

Epicenter coordinates	$151{,}8^0$E $44{,}763^0$N
Focal depth (km)	26
Fault length (km)	250
Fault width (km)	150
Strike angle	223
Dip angle	22
Rake angle	90
Displacement (m)	3

Calculated by the Okada formula [Okada, 1985], the tsunami source is shown in Fig. 8. The water rise in the source was 1.4 m, and the descent was 0.3 m, so that the water level difference (height) in the source was 1.7 m.

The simulation was to last 10 operation hours, enough for the wave to propagate in the Sea of Okhotsk. The numerical results were verified on the basis of tsunami observation data in the Kuril Islands, which we omit here.

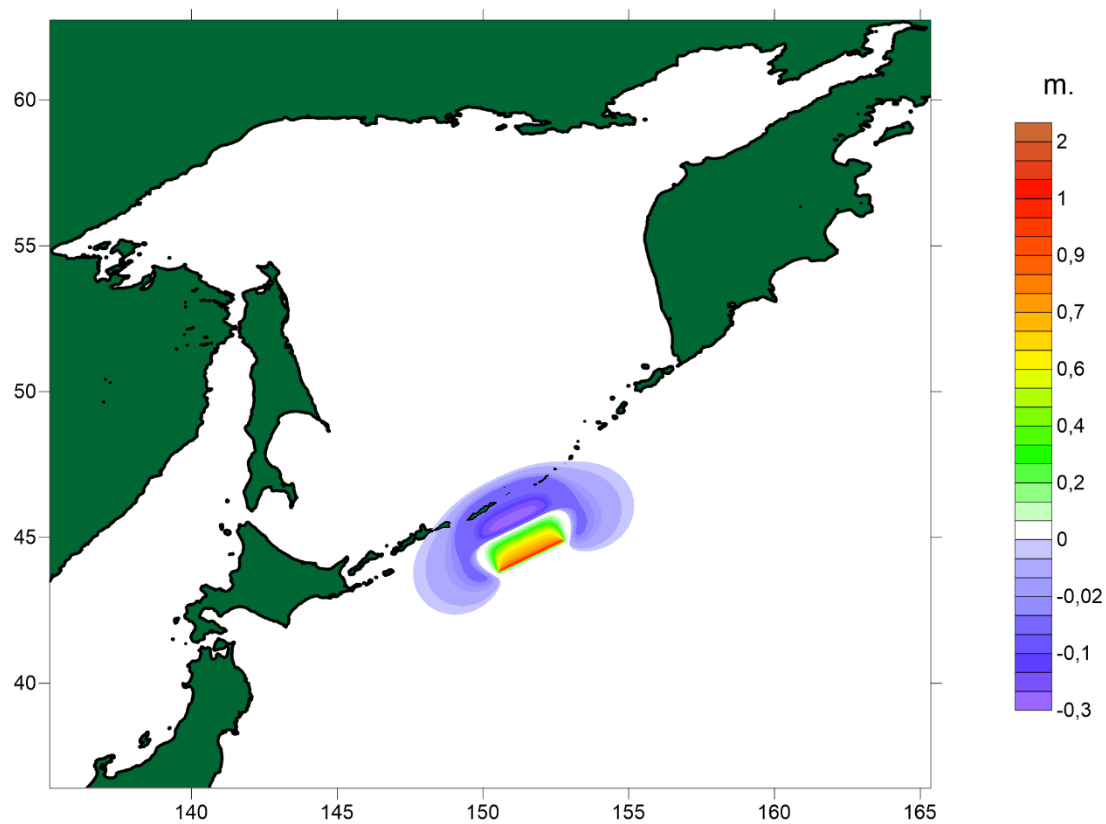

Figure 8. The computed tsunami source

Fig. 9 shows the spatial distribution of the tsunami amplitude for the entire calculation area. It is seen, as expected, that the bulk of the tsunami energy is in the Pacific Ocean where it is dispersed. In the Kuril Islands the largest amplitudes according to numerical calculation results are from the Pacific side in the vicinity of the source and large islands. In the Sea of Okhotsk, there are three areas where tsunamis most intensively manifested themselves: the Sakhalin southern and eastern coast, the Sea of Okhotsk northern coast and the Kamchatka Peninsula western coast. The same areas of increasing tsunami intensity are also noted for other tsunami events [Kostenko et al, 2015; Zaytsev et al, 2016, 2017]. On the Sakhalin coast, the largest values of tsunami amplitudes were shown on the east and south-east coasts, according to numerical calculations. In the Tatar Strait (the Sakhalin Island western coast) tsunami waves were less intense, especially in the central and northern parts.

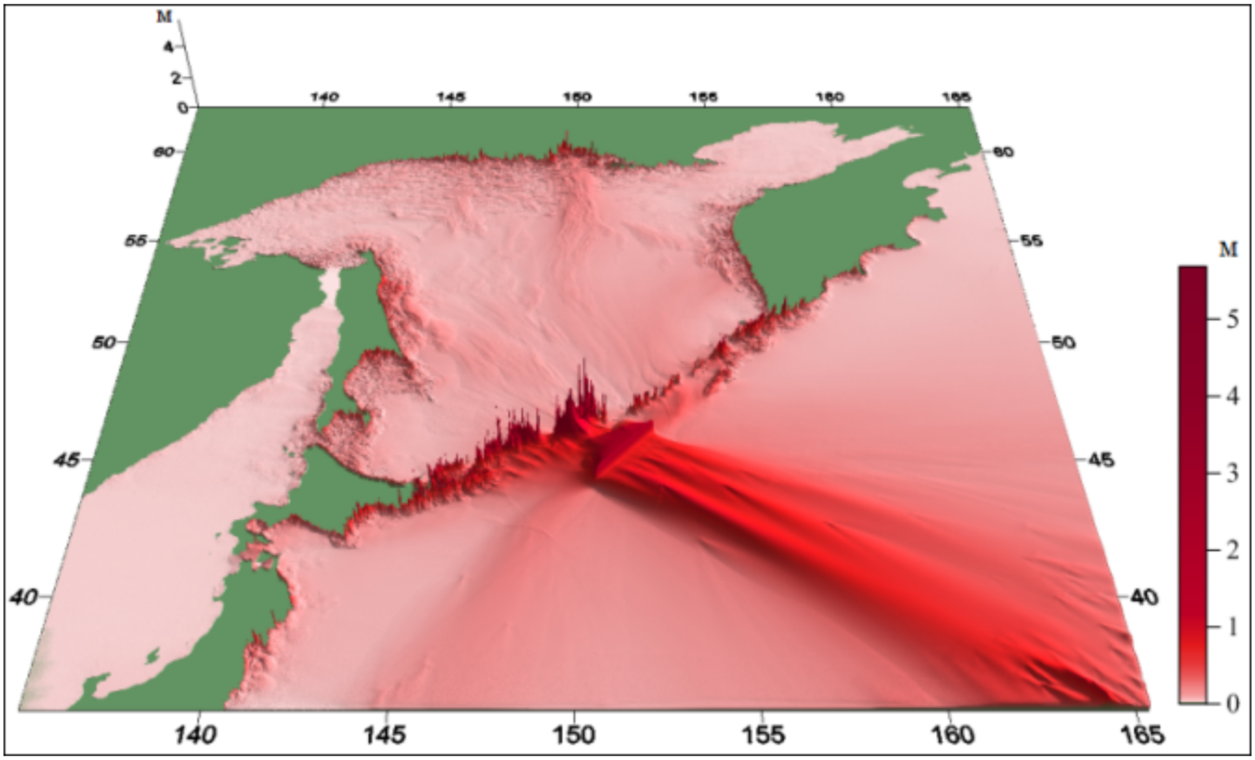

Figure 9. Distribution of the 1963 Urup tsunami maximal wave amplitudes

Let us discuss in more detail the tsunami quantitative characteristics. Fig. 10 shows the maximum value calculated distribution of tsunami amplitudes along the Coast of Sakhalin Island. On the northeastern coast of Sakhalin, according to observations, the tsunami height in the settlement of Katangli was 0.4 m. The maximum values of the tsunami amplitudes are on average 0.2-0.5 m, according to the numerical calculation results. According to observations in Terpeniya Bay in the town of Poronaisk, the tsunami wave height reached 0.3 m. The maximum amplitudes of tsunami wave in Terpeniya Bay and on the Sakhalin southeast coast, according to the numerical calculation results, are in the range 0.2-0.8 m. The highest values of wave amplitudes are on the Tonino-Aniva Peninsula east coast (0.4-0.6 m) and in the upper part of Terpenia Bay (0.7-0.8 m).

According to observations on the western coast of the island, the tsunami manifested itself in Nevelsk (0.15 m) and in Kholmsk (0.1 m), which is consistent with numerical calculations. On the coast of the Tatar Strait, the largest wave amplitudes are found in the south-eastern part of Sakhalin in the area of the Strait of La Perouse, according to the numerical simulation. From there the most part of the waves were hardly manifested themselves, according to the numerical simulation.

On the Sakhalin northern coast the measurements were not carried out, but according to the numerical simulation, the tsunami wave height here did not exceed 0.15 m.

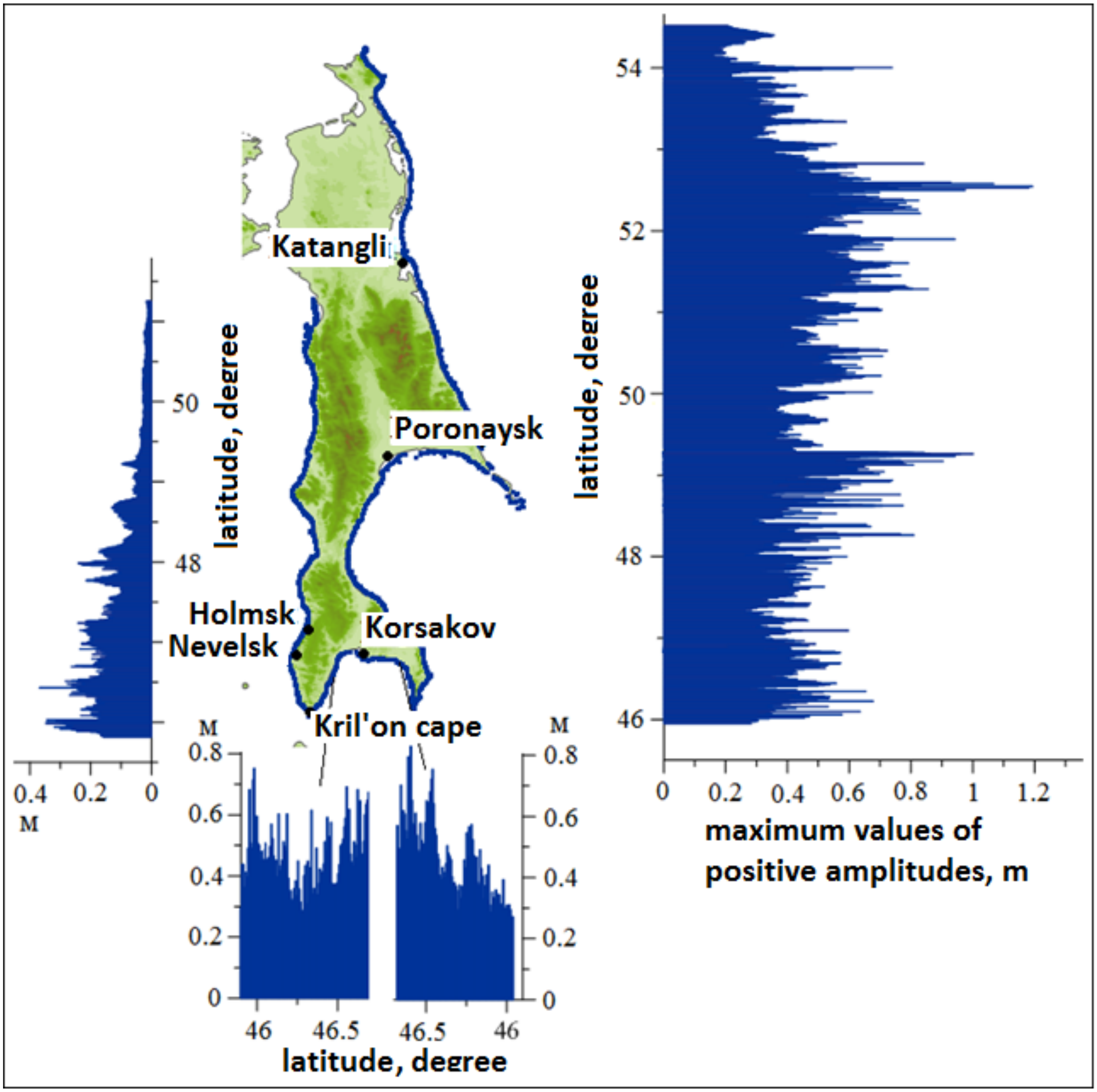

Figure 10. Distribution of the maximum wave amplitudes along the coast of Sakhalin.

Fig. 11 shows travel times of tsunamis of the leading wave (a) and wave of maximal amplitude (b). Tsunami waves approach the south-east coast of Sakhalin 1 hr after earthquake and after 2-3 hrs the wave comes to the main cities of Sakhalin (Poronaisk, Kholmsk). After 10 hrs waves reached all coastal locations on Sakhalin.

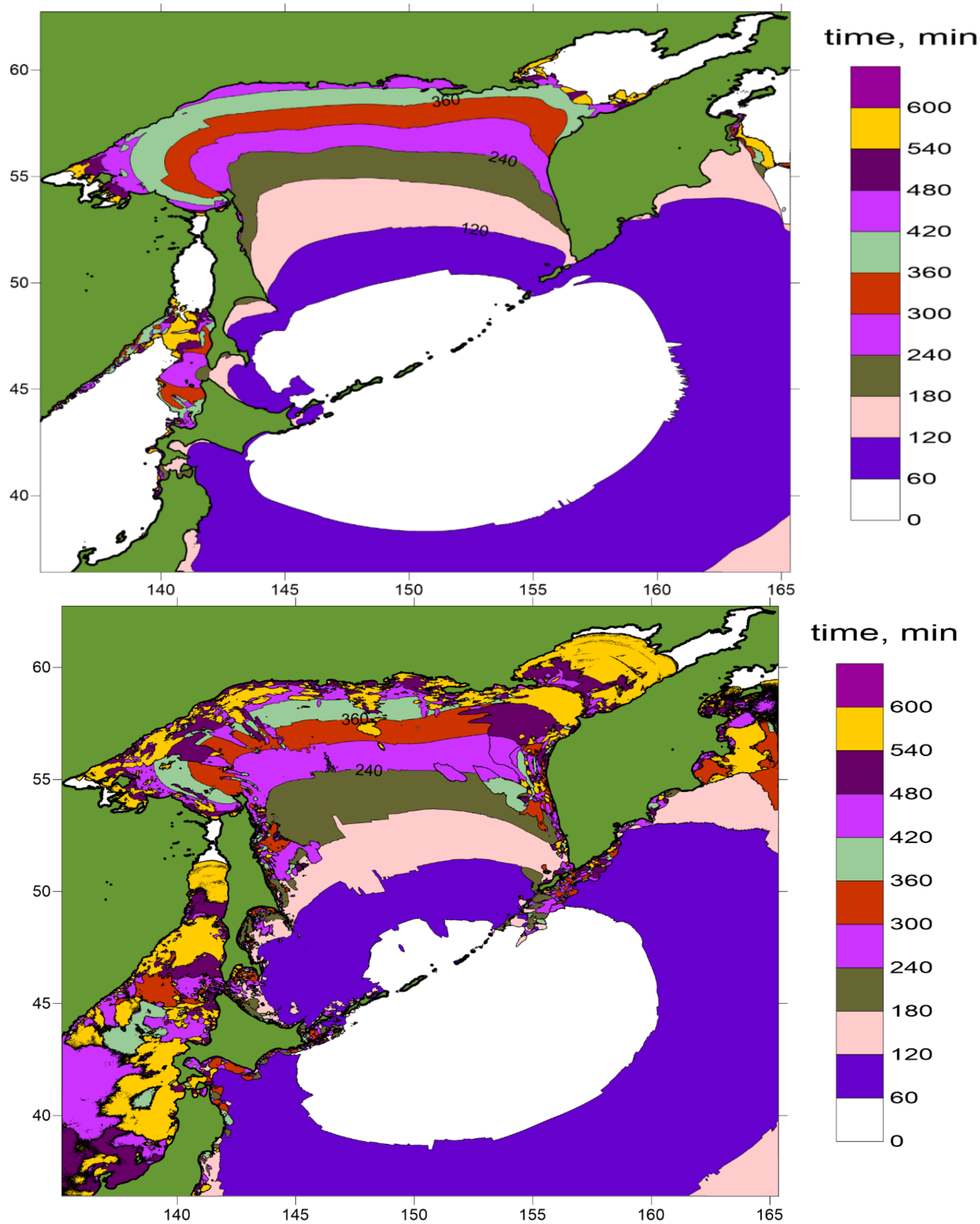

Figure 11. Computed travel time: a) leading wave, b) wave of maximal amplitude

Computed tide-gauge records in several coastal locations where tsunami was recorded are displayed in Fig. 12.

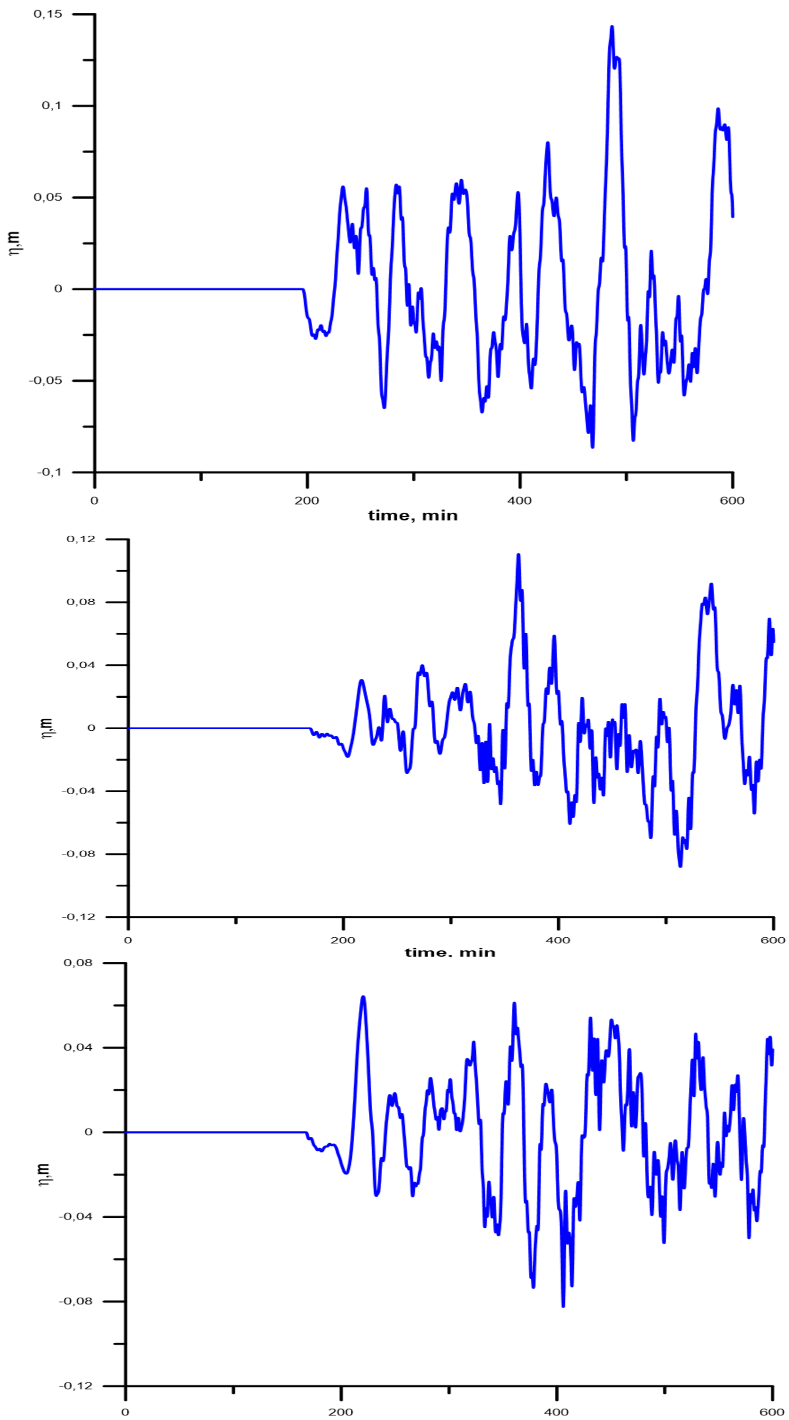

Figure 12. Computed tide gauge records of 1963 tsunami in Katangli (above), Korsakov (middle), and Krilion Cape (below)

According to simulation the tsunami began from the ebb phase. Then the series of large waves in the time period of approximately 5 hrs is clearly visible on mariograms. Let us compare the observed and computed tide gauge records in Katangli (Figs. 3 and 12). Both mariograms begin from the negative wave. The wave of maximal amplitude comes 5 hrs after the earthquake according to both, observation and computation. So, the agreement between mariograms is very good. According to the observations a wave of maximal amplitude arrives in 3 hrs after the earthquake in Korsakov and this corresponds to the computations. On the records in Krilion Cape the wave of maximal amplitude is not clearly selected in both, in observations and computations. So the agreement between observations and computations is quite good.

Similar tide gauge records are computed for some other coastal locations (Fig. 13). Unfortunately, we could not compare here tide gauge records because only visual observations are available for these locations.

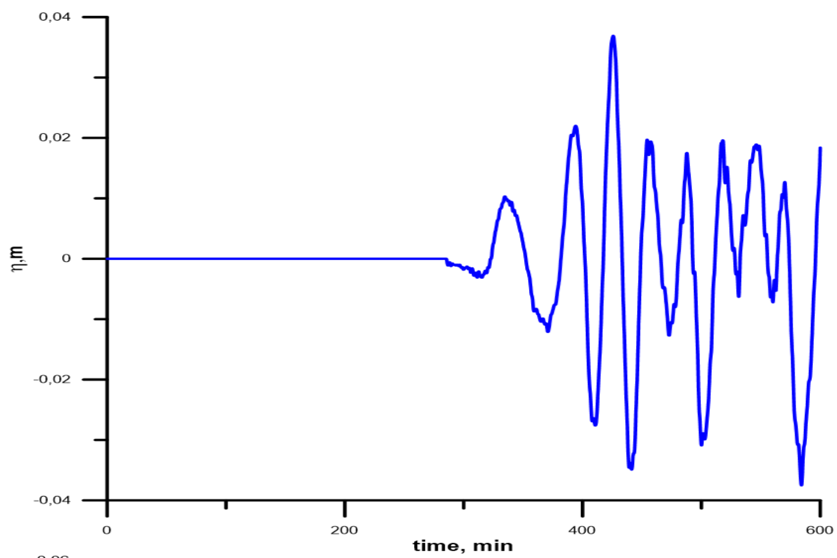

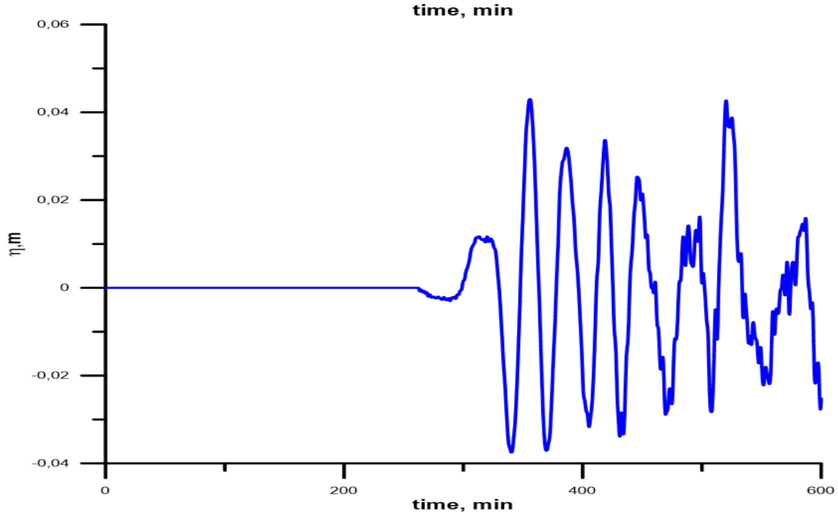

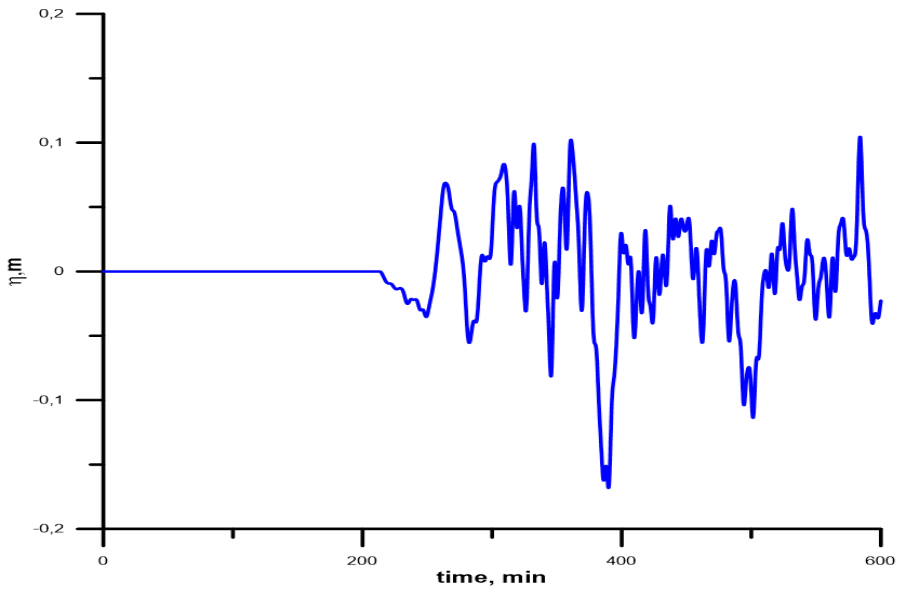

Figure 13. Computed tide gauge records of 1963 tsunami in Kholmsk (above), Nevelsk (middle), and Poronaisk (below)

Table 3. Observed and computed wave heights on Sakhalin

Coastal location	Tsunami height according to observations, m	Tsunami height according to numerical simulations, m
Katangli settlement	0,4	0,5
Poronaisk	0,3	0,6
Korsakov	0,4	0,6
Cape Krilion	0,4	0,4
Nevelsk	0,15	0,26
Kholmsk	0,1	0,3

The 1963 Urup tsunami wave heights, observed and calculated for the coastal locations of Sakhalin, are presented in Table 3 and are shown in Fig. 14. They show that the calculated wave heights are slightly higher than those observed, which can be considered a good result.

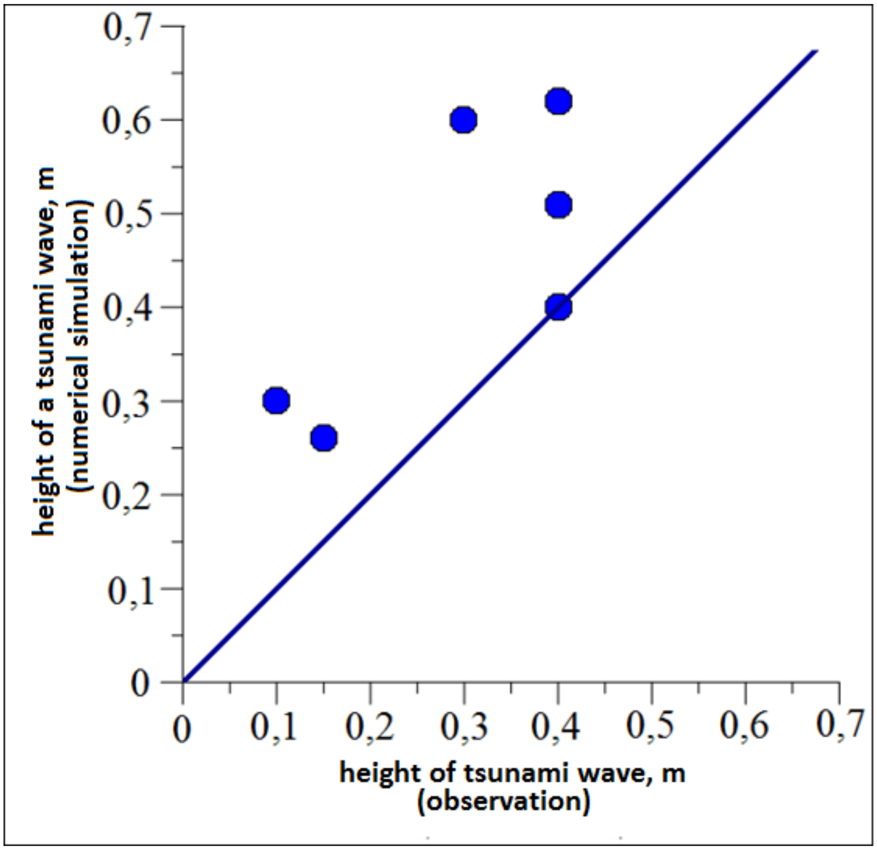

Figure 14. Comparison of the observed and computed 1963 tsunami wave heights on Sakhalin

6. CONCLUSION

About 30 tsunami events have been recorded on the island of Sakhalin, located in the Sea of Okhotsk, for the whole history of observations [Zaytsev et al, 2017]. The strongest impact on Sakhalin was made by the tsunami caused by the earthquake of October 13, 1963 at 05:17:51 GMT in the area of Urup (the Kuril Islands).The magnitude of this earthquake is 8.1 (according to some data, Mw = 8.5). Its location near the Kuril large straits Vries and Bussol contributed to a greater tsunami wave penetration into the Sea of Okhotsk, and, in particular to Sakhalin Island. The tsunami wave heights on Sakhalin did not exceed 0.4 m, while in the source they were 4-5 m high. This article summarizes tsunami instrumental observation data on Sakhalin.

Tsunami propagation numerical modeling in the framework of nonlinear shallow water theory has also been performed. The earthquake source described in [Ioki and Tanioka, 2008] was chosen. The tsunami source is calculated with the help of Okada's solution [1985].

The computed results are verified by the observation data on the Kuril Islands. Tsunami characteristics on the Coast of Sakhalin Island are also computed. Numerical modeling allowed us to explain the observations of the 1963 Urup tsunami, confirm the chosen earthquake model, and also to estimate the tsunami heights in the places where observations were not conducted.

ACKNOWLEDGEMENTS

This study was initiated in the framework of the state task programme in the sphere of scientific activity of the Ministry of Education and Science of the Russian Federation (projects No. 5.4568.2017/6.7 and No. 5.5176.2017/8.9), grant of the President of the Russian Federation NSh-6637.2016.5 and RFBR grants 16-55-52019 and 17-05-00067.

BIBLIOGRAPHY

1. Baranova, N.A., Kurkin, A.A., Mazova, R., and Pararas-Carayannis, G. Comparative numerical simulation of the Tohoku 2011 tsunami. Science of Tsunami Hazards, 2015, vol. 34, No. 4, 212-230.
2. Dilmen, D. I., Kemec, S., Yalciner, A. C., Duzgun, S., and Zaytsev, A. Development of a tsunami inundation map in detecting tsunami risk in Gulf of Fethiye, Turkey. Pure and Applied Geophysics, 2015, vol. 172, 921-929.
3. Iida, K., D.C. Cox, and Pararas--Carayannis, G., Preliminary Catalog of Tsunamis Occurring in the Pacific Ocean. Data Report No. 5. Honolulu: Hawaii Inst. Geophys. Aug. 1967.
4. Imamura, F. Tsunami Numerical Simulation with the staggered leap-frog scheme (Numerical code of TUNAMI-N1). School of Civil Engineering, Asian Inst. Tech. and Disaster Control Research Center, Tohoku University. 1989
5. Ioki, K., and Tanioka, Y. Tsunami waveform analyses of the 1963 Kurile Islands earthquake. American Geophysical Union, Fall Meeting 2008, abstract #OS43D-1319. 2008.
6. Kaistrenko, V., Razjigaeva, N., Kharlamov, A., and Shishkin, A. Manifestation of the 2011 Great Tohoku tsunami on the coast of the Kuril Islands: A tsunami with ice. Pure and Applied Geophysics, 2013, vol. 170, 1103-1114.
7. Kostenko, I., Yalciner, A., Kurkin, A., Pelinovsky, E., and Zaytsev, A. Tsunamis in the Sea of Okhotsk: facts and modelling. Proc. Twelfth Int. Conf. on the Mediterranean Coastal Environment Medcoast -2015 (06-10 October 2015, Varna, Bulgaria). Ed. E. Ozhan. 869-880.
8. Kostenko, I.S., Kurkin, A.A., Pelinovsky, E.N., and Yalciner, A. The influence of the Kuril Islands on the penetration of tsunamis into the Sea of Okhotsk (on the example of the Japan tsunami on March 11, 2011). Izvestiya, Atmospheric and Ocean Physics, 2016, vol. 52, No. 1, 89-100.
9. Kurkin, A.A., Pelinovsky, E.N., Choi, B.H., and Lee, J.S. A comparative estimation of the tsunami hazard for the Russian coast of the Sea of Japan based on numerical simulation. Oceanology, 2004, vol. 44, No. 2, 163-172.
10. Levin, B.V., and Nosov, M.A. Physics of Tsunami. Springer, 2016
11. Okada, Y. Surface deformation due to shear and tensile faults in a half-space. Bulletin of the Seismological Society of America. 1985, vol. 75(4), 1135-1154.

12. Ozer,, C.S., Yalciner, A.C., and Zaytsev, A. Investigation of tsunami hydrodynamic parameters in inundation zones with different structural layouts. Pure and Applied Geophysics, 2015, vol. 172, 931-952.
13. Pararas-Carayannis, G., Catalog of Tsunamis in the Hawaiian Islands. World Data Center A-Tsunami U.S. Dept. of Commerce Environmental Science Service Administration Coast and Geodetic Survey, May 1969. Data Report Hawaii Inst.Geophys. Jan. 1968.
14. Pararas-Carayannis, G. The November 4, 1952 Kamchatks Earthquake and Tsunami. (Excerpts from the archives to the Catalogs of Tsunami in the Hawaiian Islands. World Data Center A- Tsunami U.S. Dept. of Commerce Environmental Science Service Administration Coast and Geodetic Survey, 1969.
15. Pararas-Carayannis, G. and Calebaugh P.J., Catalog of Tsunamis in Hawaii, Revised and Updated , World Data Center A for Solid Earth Geophysics, NOAA, 78 p., March 1977.
16. Pararas-Carayannis, G. The Earthquake and Tsunami of October 4, 1994 in the Kuril Islands (Tectonic Setting of the Northern Japan/Kuril Island Region), 1994. http://www.drgeorgepc.com/Tsunami1994RussiaKurils.html
17. Pararas-Carayannis, G. The Earthquake and Tsunami of 15 November 2006 in the Kuril Islands. 2006. http://www.drgeorgepc.com/Tsunami2006Kurils.html
18. Pelinovsky, E.N. Tsunami Wave Hydrodynamics. Institute Applied Physics Press, Nizhny Novgorod. 1996 (in Russian).
19. Schetnikov, N.A. Tsunami. Moscow: Nauka, 1981 (in Russian).
20. Schetnikov, N.A. Tsunami on the coast of Sakhalin and the Kuril Islands according to the tide gauge data of 1952-1968. – Vladivostok: FEB RAS, 1990 (in Russian).
21. Shevchenko, G.V., Ivelskaya, T.N., Kovalev, P.D., Kovalev, D.P., Kurkin, A.A., Levin, B.V., Likhacheva, O.N., Chernov, A.G., and Shishkin, A.A. New data about tsunami evidence on Russia's Pacific coast based on instrumental measurements for 2009-2010. Doklady Earth Sciences, 2011, vol. 438, No. 2, 893-898.
22. Shevchenko, G.V., Ivelskaya, T.N., and Kaistrenko, V.M. Tsunami on the Kuril Islands. Features of manifestation and measures to reduce risk. - Yuzhno-Sakhalinsk: IMGiG FEB RAS, 2012 (in Russian).
23. Shuto, N., Goto, C., and Imamura, F. Numerical simulation as a means of warning for near field tsunamis. Coastal. Engineering in Japan, 1990, vol. 33, No. 2, 173-193.
24. Solovyev, S.L. Earthquakes and tsunami on October 13 and 20, 1963 on the Kuril Islands. Yuzhno-Sakhalinsk – SakhKNII, 1965 (in Russian).
25. Solovyev, S.L. Basic data on the tsunami on the Pacific coast of the USSR, 1737-1976. In: The study of the tsunami in the open ocean. Moscow: Nauka, 1978, 61-136 (in Russian).
26. Yalciner, A.C., Pelinovsky, E., Zaytsev, A., Kurkin, A., Ozer, C., Karakus, H., and Ozyurt, G. Modeling and Visualizations of tsunamis: Mediterranean Examples. Tsunami and Nonlinear Waves // (Ed: Anjan Kundu), Springer. 2007. P. 2731-2839.
27. Yalciner, A., Zahibo, N., Insel, I., Dilmen, D.I., Zaytsev, A., Chernov, A., Ozer, C., and Pelinovsky, E. Understanding the possible effect near far field tsunamis on Lesser Antilles by numerical modelling. The Open Oceanography Journal, 2010, № 4, 50-57.

28. Zaitsev, A.I., Kovalev, D.P., Kurkin, A.A., Levin, B.W., Pelinovsky, E.N., Chernov, A.G., and Yalciner, A. The Nevelsk tsunami on August 2, 2007: Instrumental data and numerical modelling. Doklady Earth Sciences, 2008, vol. 421, No. 1, 867-870.
29. Zaitsev, A.I., Kovalev D.P., Kurkin, A.A., Levin B.V., Pelinovskii E.N., Chernov A.G., and Yalciner A. The tsunami on Sakhalin on August 2, 2007: Mareograph evidence and numerical simulation. Russian J Pacific Geology, 2009, vol. 3, No. 5, 437 – 442.
30. Zaitsev, A.I., Kurkin, A.A., Levin, B.V., Pelinovsky, E.N., Yalciner, A., Troitskaya, Yu.I., and Ermakov, S.A. Numerical simulation of catastrophic tsunami propagation in the Indian Ocean. Doklady Earth Sciences, 2005, vol. 402, No. 4, 614-618.
31. Zaytsev, A.I., Pelinovsky, E.N., Kurkin, A.A., Kostenko, I.S., and Yalciner, A. The possibility of tsunami in the Sea of Okhotsk caused by deep-focus earthquakes. Izvestiya, Atmospheric and Ocean Physics, 2016, vol. 52, No. 2, 217-224.
32. Zaytsev, A.I., Kostenko, I.S., Kurkin, A.A., and Pelinovsky, E.N. Tsunami on Sakhalin Island: observations and numerical modeling. – Yuzhno-Sakhalinsk: NNGTU, 2017. 121 p (in Russian).